

SCHEDULING AND ROUTING FOR TIMETABLE-BOUND URBAN AIR MOBILITY OPERATIONS

Adler Edsel[1], William A. Crossley[2] & Daniel A. DeLaurentis[3]

[1]Graduate Research Assistant, School of Aeronautics and Astronautics, Purdue University
[2]Uhrig & Vournas Head and Professor of Aeronautics and Astronautics, Purdue University
[3]Bruce Reese Professor of Aeronautics and Astronautics, Purdue University

Abstract

Passenger-carrying Urban Air Mobility (UAM), based on their service concept, can generally be categorized as either on-demand or timetable-bound (i.e., based on a pre-defined schedule). While most studies focus on on-demand UAM operations, scheduled UAM services may also be viable if passenger demand is sufficient to support such services and if scheduling reduces non-revenue repositioning flights. This study developed a modeling framework for daily scheduled UAM operations by adapting airline scheduling and aircraft routing techniques to a reservation-based, timetable-bound service. The modeling framework begins with a maximum-throughput scheduling approach that generates departure and arrival slots at each aerodrome over a 24-hour simulation horizon, after which passenger demand is assigned to these slots to produce a timetable of feasible UAM flights. This is followed by a tail-number assignment problem formulated as a minimum-cost flow to minimize the fleet size required to fully cover the resulting flight schedule. Additional repositioning flights are introduced as necessary, providing opportunities to accommodate more passenger demand. We consider several distinct three- and four-aerodrome networks in the Chicago metropolitan area in the United States and apply the schedule-based UAM model to these networks. The resulting scheduled UAM services carried approximately 3,000 passengers per day across all aerodrome network scenarios considered. Collectively, these results demonstrate that the overall scheduled UAM model can be applied across aerodrome networks of distinct sizes and configurations while maintaining a repeatable daily schedule of operations and respecting aerodrome throughput and aircraft-on-ground capacity constraints.

Keywords: urban air mobility, airlines, scheduling, aircraft routing, networks

1. Introduction

Urban Air Mobility (UAM) is an emerging mode of intra-urban air transportation that uses small electric vertical takeoff and landing (eVTOL) aircraft to transport passengers (and cargo) within and around metropolitan areas [1]. For passengers, UAM aims to shorten travel times compared to existing ground transportation modes, potentially offering benefits for travel within and around cities with severe road congestion or limited transit options [2].

UAM operations would likely rely on ground infrastructure capable of supporting eVTOL aircraft such as airports, heliports, seaplane ports, and purpose-built vertiports, collectively referred to as aerodromes. These form part of a multimodal transport system in which passengers connect between UAM services and other modes for first- and last-mile travel [3]. In the United States (U.S.), UAM ecosystems are in active development driven by both government agencies and industry partners. This includes city-level implementation efforts in Dallas [4] and Orlando [5], and partnerships between airlines and original equipment manufacturers (OEMs) such as Delta Air Lines with Joby Aviation [6] and United Airlines with Eve Air Mobility [7] and Archer Aviation [8]. On the regulatory side, the U.S. Federal Aviation Administration (FAA) released new planning and design standards for eVTOL-aircraft-capable aerodromes in late-2024 [9], and a coalition of national aviation authorities

https://doi.org/10.71945/icas2026_0103

announced a multilateral certification roadmap for UAM operations in mid-2025 [10]. More recently, the U.S. FAA selected eight proposals from state and municipal agencies in conjunction with industry partners in early-2026 as part of their AAM and eVTOL Integration Pilot Program [11].

UAM service models generally fall into two categories: on-demand and scheduled [12]. On-demand UAM would resemble existing ride-hailing services, whereby passengers request flights in real time through an operator or platform [13, 14]. However, given possible constraints on aircraft availability as well as infrastructure for eVTOL aircraft and UAM operations, true on-demand operations may be difficult to realize. Instead, scheduled (or timetable-bound) UAM services, as envisioned by Boeing and Wisk in their Concept of Operations document [15], could offer regularly timed departures similar to those offered by commercial airlines or rapid-transit systems. While most prior studies assume on-demand UAM operations, recent work has begun to explore scheduled concepts, including hub-and-spoke or hybrid models that combine schedule-based and on-demand flights [16, 17].

However, current literature offers limited modeling of purely scheduled UAM services despite growing interest. To address this gap, this paper presents a modeling framework for a hypothetical profit-seeking operator conducting scheduled UAM services in the Chicago metropolitan area. Adapting several features of established airline scheduling and aircraft routing techniques, the proposed scheduling-and-routing model simulates a reservation-based, commercial-airline-like service concept and is used to assess aerodrome capacity constraints, UAM demand capture, the fleet size required to fulfill this demand, and the prevalence of deadhead or repositioning flights relative to passenger-carrying flights. This extends the work presented in Ref. [18], incorporating several updates and enhancements to the underlying datasets, scheduling-and-routing methodology, and aerodrome networks. However, unlike Ref. [18], the present work focuses exclusively on commercial-airline-like operations.

Overall, we seek to address the following research questions:

1. How can current methods of commercial airline planning, such as in scheduling and aircraft routing, be adapted to timetable-bound UAM operations?
2. How might a profit-seeking operator providing scheduled UAM services perform across aerodrome networks of varying size under aerodrome capacity constraints, as measured by passenger throughput, aircraft fleet size, and the frequency of repositioning flights?

2. Background and Prior Research

Most studies in the existing literature involving UAM operations or concepts of operations have modeled, or implicitly assumed, on-demand operations. Bennaceur et al. [19] proposed a mixed-integer linear program for passenger pooling, aircraft scheduling, and maintenance-aware routing. Their approach first assigns passenger requests to pooled flights and then solves a routing-and-recharging problem that ensures feasibility while establishing operator- and passenger-oriented performance metrics. Although the general structure of assigning passengers to flights and then assigning aircraft to operate those flights is similar to the approach used in this work, the present study focuses on daily commute trips and pools passengers based on effective-cost preferences to generate a feasible set of UAM flights.

Yang et al. [20] developed a mixed-integer bilinear programming model for ride-sharing-enabled on-demand AAM operations, jointly solving aircraft assignment and detailed flight-path planning across multiple travel modes. Their high-fidelity model is computationally intensive, with reported run times exceeding 1,700 seconds for only 30 passengers, making such resolution impractical for applications involving passenger volumes in the order of thousands. Wei et al. [21] formulated a mixed-integer program to obtain optimal on-demand UAM schedules under travel time uncertainty and destination aerodrome capacity limits in a star-branch network. Their approach differs from the simultaneous

demand-assignment and scheduling structure used in this work and is oriented toward on-demand rather than timetable-bound operations.

In contrast to the extensive focus on on-demand operations, relatively few studies investigate scheduled or hybrid UAM services. Shihab et al. [16] proposed a mixed-integer quadratic programming model for scheduling and dispatching under on-demand, schedule-based, and hybrid UAM operations. Their formulation adjusts constraints to vary the mix of on-demand and scheduled service and identifies potential performance metrics such as profit, demand served, and passenger delay. The present study, on the other hand, focuses solely on scheduled UAM operations.

Kang and Kim [17] examined schedule-based UAM in a hub-and-spoke network in Seoul, South Korea, comparing reservation-based and first-come, first-served models using discrete-event simulation. Their results indicate lower delays and shorter connection durations under the reservation-based service. In contrast, the present study focuses solely on a reservation-based commercial-airline-like model while considering smaller three- and four-aerodrome networks and assuming nonstop passenger segments on UAM without connections.

Lastly, the work demonstrated in Ref. [18] demonstrates that a commercial-airline-like model for scheduled UAM services carries more passengers on fewer flights, whereas a rapid-transit-like model required a slightly smaller fleet of aircraft but resulted in more empty flights and fewer passengers carried. The present study adopts and extends the commercial-airline-like model.

3. Study Design and Setup

At the foundation of this study is a previously developed mode choice framework that (a) generates a list of daily commute trips within a given metropolitan region and (b) models their individual travel mode preferences. Several of the features and assumptions that underpin the mode choice framework, such as the *effective cost* metric that hinges upon the economic rationality of the traveler, have been adapted and incorporated into the present study and are described in detail throughout this section. Illustrated in Fig. 1, the mode choice framework broadly considers two specific door-to-door travel modes: the car mode, which involves a singular nonstop ground segment between an individual's origin and destination; and the UAM mode, which itself involves three segments:

- a first-mile ground segment between an individual's origin and the aerodrome that is closest to their origin, referred to as their *departure aerodrome*,
- a UAM flight segment between their departure aerodrome and their *arrival aerodrome* that is closest to their destination,
- and a last-mile ground segment between their arrival aerodrome and their final destination[1].

The following subsections provide an overview of the input data sources, processes, and assumptions in the mode choice framework.

3.1 Generation of Daily Commute Trips

The study presented in this paper draws upon a comprehensive dataset of intra-urban commute trips for a representative day. This dataset, obtained and synthesized from various sources as described by Maheshwari et al. [22], serves as the basis for subsequent mode choice analyses and the modeling of scheduled UAM operations. Given the geographic extent of a metropolitan region of interest, the trip generation process begins by leveraging Longitudinal Employer-Household Dynamics (LEHD) Origin-Destination Employment Statistics (LODES) data from the U.S. Census Bureau [23], which provide pairs of home and work locations, or *employment links*, for all individuals with a primary workplace. Subsequently, each individual is associated with two unidirectional origin-destination employment links: one with a home location origin and a work location destination, and another in the

[1] The terms first-mile and last-mile refer to the initial and final legs of a multimodal trip, not literal mile distances.

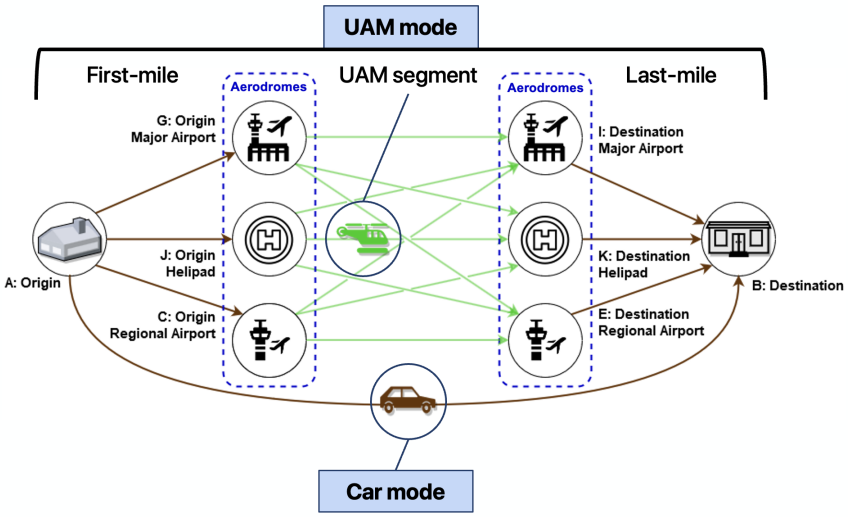


Figure 1 – Illustration of travel modes and segments modeled by the mode choice framework.

opposite direction. LODES does not distinguish between employment arrangements, such as remote versus in-person work. Nevertheless, because these employment links are contained entirely within the metropolitan region of interest, they are assumed to represent commute trips already undertaken on a weekday basis.

Next, we quantify potential travel time savings offered by different travel modes through an individual's value of time (VoT), used in the *effective cost* metric as described below. To estimate VoT, we derive household income data from census tract-level income distributions obtained from the American Community Survey (ACS) [24], conducted by the U.S. Census Bureau. Because mode choice analyses in this study center around trips to and from work, we make the assumption that the VoT of a commuting individual is equivalent to their hourly income, expressed in U.S. dollars (USD) per hour. Finally, data from the National Household Travel Survey (NHTS) of the U.S. Federal Highway Administration (FHA) [25] provide a distribution of destination arrival times.

3.2 Mode Comparisons Using the Effective Cost Metric

Given origin and destination points pertaining to all commute trips, the framework utilizes road networks provided by the Open Street Routing Machine [26] to (a) identify aerodromes closest to these points, (b) build turn-by-turn directions for all ground travel, and (c) calculate ground travel times across both the car and UAM modes. We further multiply these ground travel times by an hourly TomTom traffic congestion index [27] that corresponds to the metropolitan region of interest. Similar to previous work [18, 22, 28, 29], this study considers a notional eVTOL aircraft with a maximum passenger capacity of four, a cruise speed of 241 kilometers per hour (150 miles per hour), a nonstop range of 92.6 kilometers (50 nautical miles), and a direct operating cost of 605 USD per flight hour. For comparison, consistent with the U.S. Internal Revenue Service (IRS) 2024 standard mileage rate [30], the operating cost of the notional ground vehicle has been set at 0.42 USD per kilometer (0.67 USD per mile).

At the core of the mode choice framework employed in this study is the *effective cost* metric. The framework assumes completely rational travelers with full knowledge of the costs associated with all travel modes, who consequently select the mode with the lowest effective cost. Similarly, in calculating the effective cost, we assume that travelers bear the "operating" cost of being carried on a vehicle they find themselves in. The effective cost metric therefore comprises this operating cost and a *time cost* obtained by multiplying the total door-to-door travel duration with an individual's unique VoT. For shared UAM flights, aircraft operating costs are divided equally among passengers. Each passenger's effective cost for the UAM mode is then computed as the sum of their share of the aircraft operating cost, the cost incurred by first- and last-mile ground segments, and their total time cost.

We encourage readers to refer to [31], [32], [33], [34], [22], [29], and [35] for a more comprehensive understanding of the underlying modeling framework that enable UAM mode choice analyses.

3.3 Study Area and Aerodrome Network Scenarios

Consistent with earlier investigations of UAM demand and operational limits centered on the Chicago metropolitan area in the U.S. [22, 28, 36, 18, 37], the present study likewise focuses on the Chicago metropolitan area. To this end, the U.S. Census Bureau's American Community Survey [24] defines a geographic boundary for the Chicago-Naperville-Elgin, IN-IL Metropolitan Statistical Area (MSA) covering 17,931 square kilometers (6,923 square miles) with a 2024 population estimate of just over 9.4 million [38]. This Chicago MSA forms part of a larger combined statistical area (CSA) which joins adjacent MSAs and micropolitan statistical areas. This CSA, referred to as the Chicago-Naperville, IN-IL-WI CSA, encompasses 27,542 square kilometers (10,634 square miles) and has a 2024 population estimate of nearly 10 million [39].

The aforementioned studies utilized the Chicago-Naperville, IN-IL-WI CSA. Given the geographic extent of the aerodrome networks considered in this study, discussed below, as well as the desire to establish a network definition more consistent with the notion of intra-urban travel and UAM, the present study instead adopts the Chicago-Naperville-Elgin, IN-IL MSA as its region of interest. Because the counties included in the CSA but excluded from the MSA lie beyond the nonstop range of the notional eVTOL aircraft relative to the aerodrome networks utilized in this study, this change is not expected to materially affect the resulting UAM demand. Using 2023 LODES data [23], the most recent LODES dataset available at the time of publication, we determine that the Chicago-Naperville-Elgin, IN-IL MSA, hereafter referred to as the Chicago metropolitan area, contains 8,460,586 daily intra-urban commute trips, split equally between home-to-work and work-to-home trips.

This study considers the same three-aerodrome network in the Chicago metropolitan area used in Sells et al. [29] and Ref. [18]. This three-aerodrome (3AD) network is composed of the Chicago O'Hare International Airport (KORD) [40], a major commercial airport; the Vertiport Chicago FBO (43IL) [41], located relatively close to downtown Chicago; and DuPage Airport (KDPA) [42], representing a location adjacent to a community or residential area.

To assess the scalability of the schedule-based UAM model described in the following section, the study also considers two distinct four-aerodrome network scenarios formed by augmenting the 3AD network with one of two additional aerodromes. The first four-aerodrome (4AD-1) network includes Bollingbrook's Clow International Airport (1C5) [43], and the second four-aerodrome (4AD-2) network includes Tinley Park Helistop (TF8) [44]. These additional aerodromes were selected primarily to extend UAM network coverage to the southern portion of the Chicago metropolitan area and to assess the impacts of adding a fourth aerodrome to the computations. Aerodrome siting is beyond the scope of the present study, so no claims are made as to whether 1C5 or TF8 would be the best additions to make a four-aerodrome network in Chicago. Figure 2 illustrates the network of aerodromes considered in this study.

4. Modeling Scheduled UAM Operations

Having established the region of interest, aerodrome networks for UAM services, and a framework for estimating UAM demand potential through mode choice analyses, the present study develops a schedule-based model of UAM operations representing a hypothetical operator providing timetable-bound services. Building upon the aerodrome throughput-aware schedule-based UAM model originally developed as part of Ref. [18], itself inspired by classical airline scheduling, fleeting, and routing techniques [45, 46, 47], the present study extends the methodology through several enhancements and its application through additional aerodrome network configurations.

Timetable-bound UAM operations may manifest as a service akin to that of commercial airlines, characterized by routes and flight schedules informed by anticipated travel demand while requiring

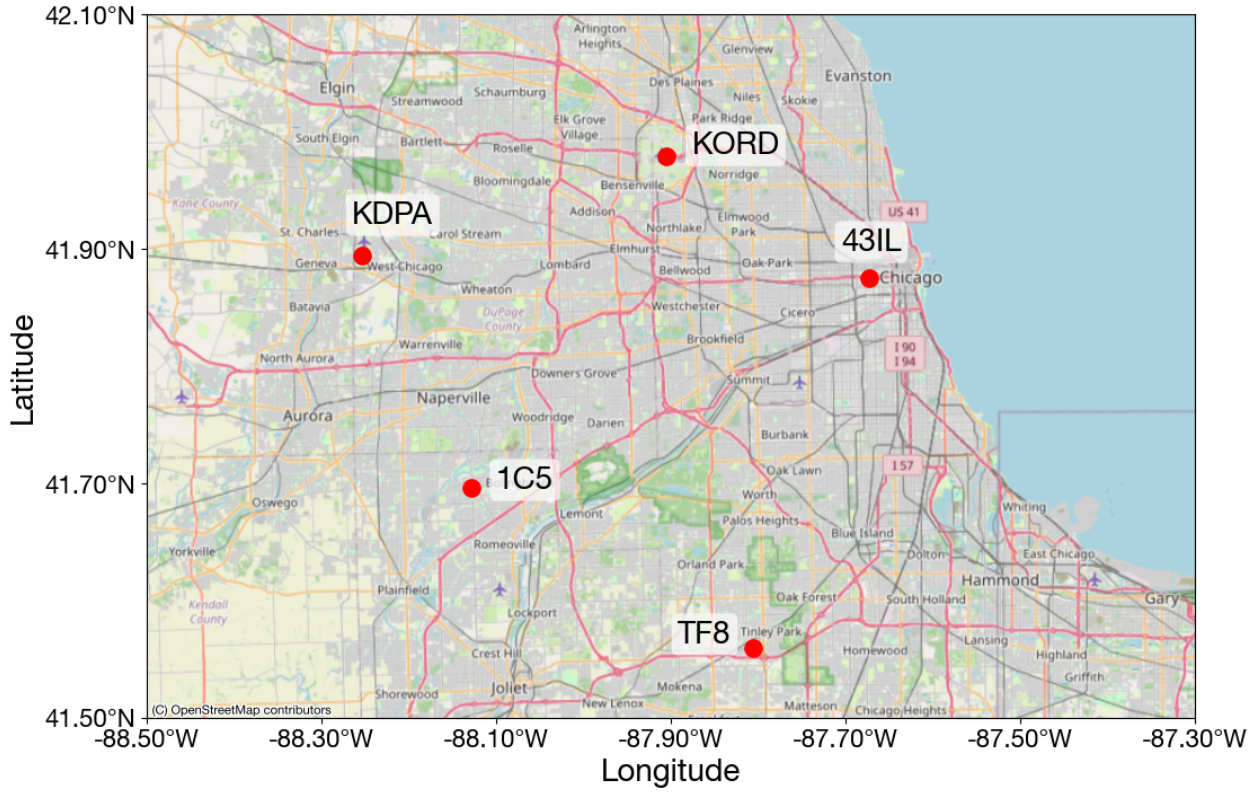


Figure 2 – Aerodromes in the Chicago metropolitan area considered in this study

passengers to make reservations or bookings in advance. Although Ref. [18] performs a comparison between commercial-airline-like and rapid-transit-like service models, the present study focuses exclusively on the commercial-airline-like model, particularly to demonstrate the scalability of the schedule-based UAM model as additional aerodromes are incorporated into the network. Across all aerodrome networks, particular interest lies in the extent of UAM demand capture, the amount of flights needed to fulfill this demand, the frequency of repositioning flights that may occasionally contain no passengers, and overall aircraft utilization while maintaining a repeatable, cyclical daily schedule of flights.

4.1 Aerodrome Concept of Operations

To account for aerodrome capacity constraints with respect to eVTOL aircraft movements, we model aerodromes as collections of touchdown-and-liftoff (TLOF) pads with associated gate capacity. Gate spaces in each aerodrome also double as storage stands and, therefore, represent the aircraft-on-ground (AOG) capacity of an aerodrome, which is crucial to flight schedule design. This study utilizes modeling described by Das Biswas et al. [36] to determine TLOF pad counts across all aerodromes. Furthermore, following general guidelines provided by Vascik [48] and utilized in Das Biswas et al. [36], a single TLOF pad corresponds to four gates and the corresponding AOG capacity of four.

To represent the movement of eVTOL aircraft into, within, and out of aerodromes, aircraft and aerodrome operations are modeled in 30-second time steps. The resulting time-expanded representation enables a discrete-event simulation employed for aerodrome slot generation, which is described in Section 4.2. We further consider various scenarios of TLOF pad independence as outlined by Vascik [48] and make the following abstractions: 1) all TLOF pads in a cluster of eight operate dependently, where aircraft movements are collectively staggered to avoid pad events occurring at the same time within this cluster; and 2) each distinct eight-pad cluster is treated in a manner independent of other clusters. In other words, simultaneous pad events may occur *between*, but not *within*, clusters of eight pads. Table 1 illustrates independent operations across two TLOF pad clusters (with a total of 16 pads), where simultaneous events may occur *between*, but not *within*, clusters of eight pads.

Table 1 – Example schedule illustrating independent pad operations between two clusters of eight pads each.

Time	Cluster 1 (Pads 1–8)	Cluster 2 (Pads 9–16)
0:00:00	Arrival (#1, Pad 1)	Arrival (#2, Pad 9)
0:00:30	Departure (#1, Pad 2)	Departure (#2, Pad 10)
0:01:00	Arrival (#3, Pad 3)	Arrival (#4, Pad 11)
0:01:30	Departure (#3, Pad 4)	Departure (#4, Pad 12)
0:02:00	Arrival (#5, Pad 5)	Arrival (#6, Pad 13)
0:02:30	Departure (#5, Pad 6)	Departure (#6, Pad 14)
0:03:00	Arrival (#7, Pad 7)	Arrival (#8, Pad 15)
0:03:30	Departure (#7, Pad 8)	Departure (#8, Pad 16)
0:04:00	Arrival (#9, Pad 1)	Arrival (#10, Pad 9)
0:04:30	Departure (#9, Pad 2)	Departure (#10, Pad 10)
⋮	⋮	⋮

A consequence of the former assumption is that, in an eight-pad cluster, four minutes separate aircraft movements in a single pad, whereas departures and arrivals are each separated by one minute collectively across the eight pads, which is consistent with Ref. [18]. The latter assumption gives rise to a situation where, should an aerodrome add a ninth TLOF pad, its aircraft movements are completely independent of those associated with the first eight TLOF pads. Although this work makes no assumption of pad separation distances, we acknowledge that a minimum pad separation of 200 feet is required for independent and simultaneous pad operations under visual flight rules (VFR) [49].

Overall, consistent with Vascik [48] and regulatory guidelines, these abstractions ensure a modular and computationally tractable formulation for the schedule design problem that can accommodate aerodromes with varying TLOF pad counts without imposing explicit geometric layouts. These abstractions further ensure that even the most stringent inter-arrival requirements under instrumental flight rules (IFR) of 90 seconds [48] are satisfied, with at least four minutes separating successive arrivals on a single pad in our modeling.

We assume embarkation and disembarkation durations of 15 and 10 minutes, respectively, along with a 30-second taxi time between TLOF pads and gates. For simplicity, these durations are assumed valid for all flights, regardless of whether they are passenger-carrying or repositioning. These durations are also associated with the beginning and end of ground and flight arcs, as illustrated in Fig. 3 taken from Ref. [18], and are utilized in the tail-number assignment methodology described in Section 4.4. We further assume that the resulting 25-minute minimum turnaround duration allows for aircraft battery charging to a state of charge (SoC) sufficient to perform any flight between aerodromes in the network. A comprehensive discussion of the rationale underlying these operational assumptions, including battery charging considerations, is provided in Ref. [18].

4.2 Throughput-Based Aerodrome Slot Generation

Having defined aircraft movements with respect to aerodromes, we utilize a discrete-event simulation to generate notional arrival and departure slots at each aerodrome based on their maximum feasible throughput, defined by its TLOF pad and gate infrastructure. This concept is analogous to takeoff and landing slot allocation at Level 3 coordinated airports such as JFK and LGA [50]. The approach to estimating throughput draws partially from Vascik [48], who characterized the number of achievable operations using an integer programming framework. Unlike that optimization-based approach, this work uses a discrete-event simulation to produce feasible slot sequences over a 24-hour period. These slots represent operational capacity and will later be matched with passenger-carrying flights.

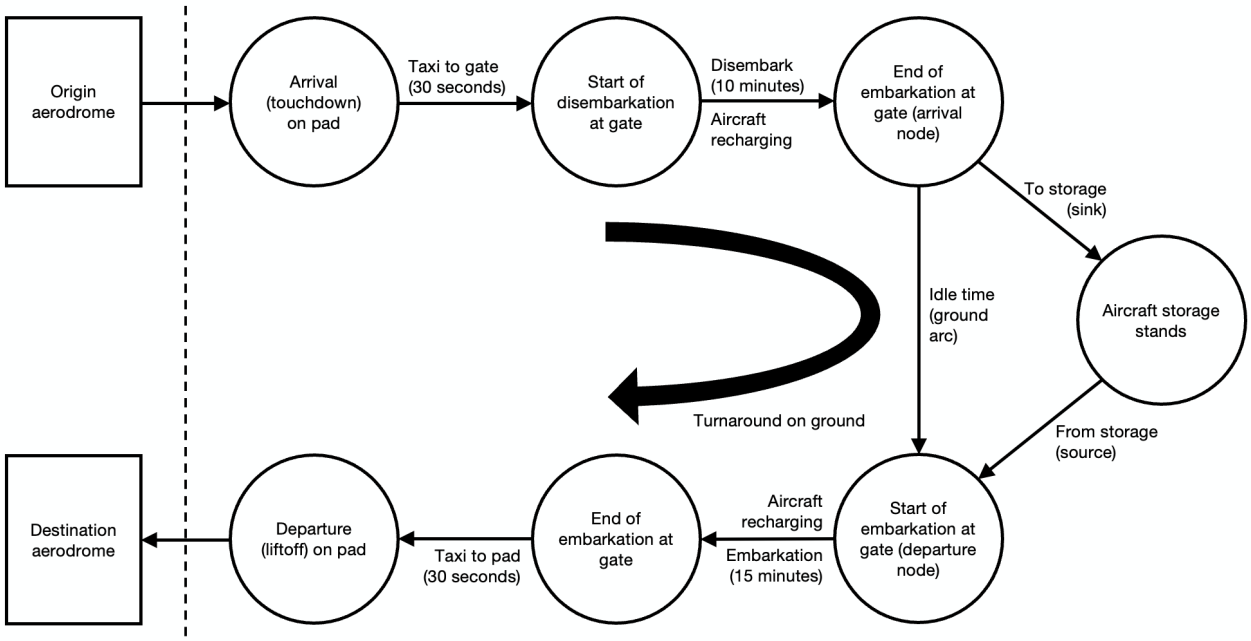


Figure 3 – Network flow representation of individual aircraft movement within aerodromes [18]

The simulation advances in 30-second increments (2880 steps over a 24-hour horizon) and incorporates operational parameters shown in Fig. 3. TLOF pads are reserved for a one-minute window centered on aircraft touchdown or liftoff, and a minimum 30-second headway is enforced between consecutive arrival events or between consecutive departure events. Additionally, arrival and departure slots are generated in alternating order to maintain slot balance and ensure that the number of departures equals the number of arrivals. This balance is necessary for respecting aircraft-on-ground (AOG) limits.

To generalize the slot-generation process to larger aerodromes, the model applies the pad-clustering structure described in Section 4.1. Slot scheduling is performed independently within each cluster and subsequently aggregated at the aerodrome level. This approach maintains computational tractability while enabling the generation of throughput-based slot schedules for aerodromes of varying sizes. The resulting output for each aerodrome is a full 24-hour record of feasible arrival and departure slots with their associated pad assignments, together with the corresponding continuous gate-occupancy intervals. These slots represent the operational envelope imposed by pad and gate counts and form the capacity constraints used in the subsequent demand scheduling and tail-number assignment stages. Table 2 summarizes slot-scheduling results for the five aerodromes included in this study, including total slots generated and the number of gates used versus those remaining vacant (and thus serving as storage stands).

Table 2 – Slot scheduling results for the five aerodromes in the Chicago metropolitan area considered in this study. The “Slots” column reports the number of arrival slots and departure slots, separately, at each aerodrome. Gate down-times between successive embarkation and disembarkation periods range from 1 to 3 minutes across all aerodromes.

Aerodrome	Pads	Slots	Gates	Used Gates	Vacant Gates
Vertiport Chicago FBO (43IL)	3	477	12	10	2
DuPage Airport (KDPA)	9	1,609	36	31	5
O’Hare Airport (KORD)	18	3,218	72	61	11
Bollingbrook’s Clow Airport (1C5)	4	715	16	14	2
Tinley Park Helistop (TF8)	2	358	8	7	1

4.3 Schedule Design: Scheduling Flights from UAM Passenger Demand

After generating aerodrome slot schedules, the next step assigns UAM-preferring individuals to feasible departure and arrival slots. This process begins with a demand dataset representing nearly 8.5 million intra-urban commute trips for a representative weekday, as described in Section 3.3. For each trip, we compute effective costs for both the car and UAM modes, assuming that eVTOL aircraft direct operating costs are shared equally among four passengers (151.25 USD per flight-hour per passenger). At this stage, we retain only individuals whose UAM-mode effective cost is lower than their car-mode effective cost, collectively referred to as the UAM-preferring demand.

For the UAM mode, each individual is already associated with a departure aerodrome, an arrival aerodrome, and a preferred departure time for the corresponding UAM flight, obtained from the mode choice framework described in Section 3.2. Given this information, each passenger is mapped to the next available departure slot at the origin aerodrome; if their preferred departure time exceeds the final slot of the day, assignment rolls to the first departure slot of the following day. Any waiting time is converted to an added time cost via the traveler's VoT. We follow the same logic for the arrival slot assignment: the passenger is matched to the earliest arrival slot at or after the calculated arrival time, and any waiting contributes additional cost.

The model also determines, for each passenger, a latest feasible UAM departure time (a "hard deadline") at which the UAM-mode effective cost would equal the car-mode cost. Every discrete departure slot between the earliest feasible slot and the hard-deadline slot is considered an acceptable option. These acceptable-slot windows form the basis for grouping passengers into four-passenger flights. Figure 4, reproduced from Ref. [18], illustrates the process by which an individual is assigned to available scheduled departure slots in a scenario where departure slots are available every four minutes.

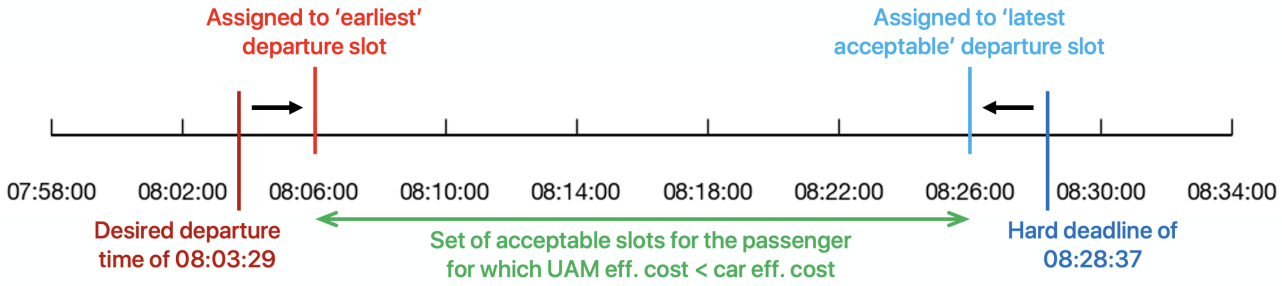


Figure 4 – A timeline network with departure slots spaced four minutes apart, demonstrating the assignment of an individual to a set of acceptable departure slots [18].

Next, passenger grouping is performed using a rule-based heuristic that assembles flights of exactly four passengers who share the same origin-destination pair and have overlapping acceptable departure-slot windows. For each OD pair, the algorithm steps chronologically through departure slots and considers passengers not yet assigned to a flight. Whenever at least four passengers share a slot in their acceptable ranges, they form a flight. If there exists between one and three candidates for a given slot, the heuristic looks back to earlier compatible passengers whose latest acceptable slot allows them to be reassigned forward. Only when four compatible passengers can be found is a flight created. Each group of four is assigned a shared departure slot, a shared arrival slot based on the duration of flight, and a unique flight identifier. This four-passenger heuristic does not create flights with fewer than four passengers, consistent with a cost structure in which each passenger is responsible for one-fourth of the aircraft's operating cost.

At this stage, because multiple candidate flights may be assigned to the same departure or arrival slot, a capacity-based conflict-resolution step is performed at the flight level. We apply a single First-In, First-Out (FIFO) rule: for each aerodrome and each departure slot, only the earliest formed flight is retained; the same rule applies to arrival slots. At aerodromes with multiple pad clusters, multiple slots

occurring simultaneously may exist, but each individual slot accommodates only one flight. Applying this conflict-resolution procedure substantially reduces the number of flights, as shown in Ref. [18]. The schedule design stage therefore yields a feasible set of flights that fit within the throughput limits of any given aerodrome network. This set is then passed directly to the tail-number assignment problem.

4.4 Aircraft Tail-Number Assignment

Following schedule design, which produces a feasible schedule of flights, the next step is to assign aircraft to these flights while minimizing the fleet size required to operate them, including any necessary repositioning. This "tail-number assignment" draws upon aircraft routing formulations found in prior studies discussed in Section 2. and in Chapter 8 of Belobaba et al. [47]. Unlike the discrete-event simulation used for schedule design, this step groups flights into ordered sequences, or "flight-strings", each representing the set of flights flown by a single aircraft over a 24-hour period [46]. This step yields a set of flight-strings that covers all scheduled flights while respecting aircraft-on-ground (AOG) capacity limits at each aerodrome and ensuring a cyclical, repeatable daily schedule. Here, we adopt several simplifying assumptions:

- All UAM operations are fully autonomous or remotely piloted, requiring no onboard crew.
- Each aerodrome offers adequate battery-charging capability.
- Only nominal operations are modeled; no disruptions or irregular events are considered.
- Each aircraft must return to its starting aerodrome at the end of the day.
- Maximum AOG capacity at each aerodrome equals its total gate count.

Given these assumptions, the tail-number assignment problem does not incorporate maintenance routing, crew scheduling, or constraints related to the availability of charging infrastructure, nor does it model required flight pairings or "throughs" as done in Barnhart et al. [46]. These simplifications allow the problem to be solved without more involved optimization frameworks, such as branch-and-price with LP relaxation, typically used in large-scale airline fleet-assignment and routing problems.

The tail number assignment process begins with the construction, for each four-passenger flight generated by the schedule design step, of two space-time nodes on a time-expanded network: 1) a departure node corresponding to the beginning of embarkation activities, and 2) an arrival node corresponding to the completion of disembarkation activities. In our modeling, departure nodes are placed 15.5 minutes prior to aircraft liftoff, whereas arrival nodes are placed 10.5 minutes following touchdown. These durations include a 30-second taxi between the gate and TLOF pad at both the departure and arrival aerodromes. Joining these space-time nodes are 1) flight arcs, which are associated with individual flights and connect departure nodes at one aerodrome with subsequent arrival nodes at another aerodrome; and 2) ground arcs, which connect arrival nodes with subsequent departure nodes at the same aerodrome, thereby representing aircraft idle time on the ground. These nodes and arcs are illustrated in Fig. 3.

Using this network representation, we formulate a minimum-cost flow problem to minimize the fleet size required to cover all scheduled flights exactly once. To this end, the formulation minimizes aircraft idle time, represented by the duration of ground arcs, with particular emphasis on aerodromes subject to more restrictive (lower) AOG capacity constraints. The resulting solution consists of a set of flight-strings, each corresponding to a sequence of flights operated by a single aircraft over the 24-hour scheduling horizon and collectively covering all scheduled flights.

We then examine opportunities to further reduce the number of flight-strings, and therefore fleet size, through the introduction of midday bridging repositioning flights. Specifically, when two flight-strings terminate and begin at different aerodromes, respectively, a repositioning flight is inserted to bridge

the two flight-strings into a single longer sequence, provided that 1) sufficient time exists for an aircraft to reposition between the two aerodromes while still accounting for prescribed embarkation and disembarkation durations, 2) feasible departure and arrival slots are still available for that repositioning flight, and 3) the resulting flight-string can still be completed within a 24-hour period. This process effectively reduces the number of flight-strings and therefore the number of aircraft required while preserving coverage of all scheduled passenger flights.

Lastly, we schedule additional end-of-day repositioning flights, as necessary, to return aircraft to their base aerodromes (i.e., the aerodrome from which each aircraft begins its flight-string). These flights, which we refer to as return-to-base (RTB) repositioning flights, are intended to restore the network-wide initial aircraft distribution and ensure day-to-day operational continuity. Extending the implementation described in Ref. [18], the present study additionally incorporates AOG capacity considerations when scheduling RTB repositioning flights. If an RTB repositioning flight scheduled for an aircraft at the earliest possible opportunity would cause the aircraft's base aerodrome to exceed its AOG capacity limit, the flight is delayed until sufficient AOG capacity becomes available, provided the aircraft can still be positioned at its base aerodrome in time to repeat its assigned flight-string on the following day.

Because these midday bridging and end-of-day RTB repositioning flights are required for operational reasons, an opportunity arises for them to carry passengers and therefore generate revenue rather than operate empty. Accordingly, as an enhancement introduced in the present study, we consider a set of yet-unassigned UAM-preferring individuals and attempts to assign them to these repositioning flights as a post-processing step. Similar to the schedule design process, individuals are considered only if their departure and arrival aerodromes, as well as their preferred departure times, are compatible with the repositioning flight. Furthermore, individuals are assigned only if their UAM-mode effective cost, including any additional time cost incurred from waiting, remains lower than their car-mode effective cost. This process slightly increases the extent of UAM-preferring demand captured by the scheduled UAM service, as demonstrated in Section 5.

Beyond these enhancements to the tail number assignment methodology, a more comprehensive discussion of its mathematical formulation, implementation, and intermediate processing steps is provided in Ref. [18].

5. Case Studies

The tail-number assignment process effectively yields a set of daily, cyclical flight-strings which minimize fleet size while fully covering all regularly-scheduled flights obtained by the schedule design step. Each flight-string is associated with a single aircraft tail number and representing a sequence of flights that include regularly-scheduled passenger flights, midday repositioning flights, and end-of-day Return-To-Base (RTB) flights.

As an illustrative example, an excerpt of the output of the tail-number assignment step can be found in Ref. [18], containing the details of consecutive flights assigned to a single aircraft. These outputs allow for extraction of a range of operational metrics for the scheduled UAM model, including the number of passengers carried, number of flights (both revenue and repositioning), load factors, fleet size, and overall aircraft utilization, which are then compared across all aerodrome networks considered. Of equal importance, however, is ensuring and demonstrating that the approach has satisfied aircraft-on-ground (AOG) capacity constraints established in Section 4.1 across all aerodromes throughout the entire 24-hour simulation horizon.

5.1 Baseline Three-Aerodrome Network

The baseline network in this study is the Chicago metropolitan area three-aerodrome (3AD) network outlined in Section 3.3. Solely on an effective-cost basis with four-passenger UAM flights, we find 39,438 individuals would prefer using UAM as part of their commute on the 3AD network; these are the commuters for whom the effective cost of using UAM is lower than the effective cost of a car-only commute. This is a small fraction of the number of commute trips inferred from LODES. Applying the schedule design process, we obtain an initial schedule of 744 four-passenger revenue flights carrying 2,976 passengers with aerodrome slot conflicts fully resolved.

Next, the tail-number assignment process determines that 45 aircraft, at a minimum, are required to fully cover these 744 passenger flights. In doing so, the process also creates 16 midday "bridging" repositioning flights and 34 end-of-day RTB flights to ensure a minimal fleet size and a repeatable, cyclical daily schedule. The model then identifies an additional 146 UAM-preferring individuals that are able to fly on 43 of the 50 repositioning flights (referred to as repositioning revenue flights), leaving only seven repositioning flights empty (referred to as deadhead flights).

Overall, the scheduled UAM service on the 3AD network was found to carry 3,122 passengers, representing only 7.92% of the overall UAM-preferring demand, on a total of 794 flights comprising 744 regular revenue (four-passenger) flights, 43 repositioning revenue flights, and 7 deadhead flights. These figures amount to a 98.3% load factor when averaged over all 794 flights.

Figure 5 illustrate cumulative counts of aircraft states as they remain at one of, or move between, the three aerodromes in the network throughout the 24-hour simulation horizon. This demonstrates the continuity of daily UAM operations, in which the number of aircraft at an aerodrome when the simulation ends is identical to that at its beginning. Aerodrome 43IL refers to Vertiport Chicago FBO, KDPA to DuPage Airport, and KORD to Chicago O'Hare International Airport.

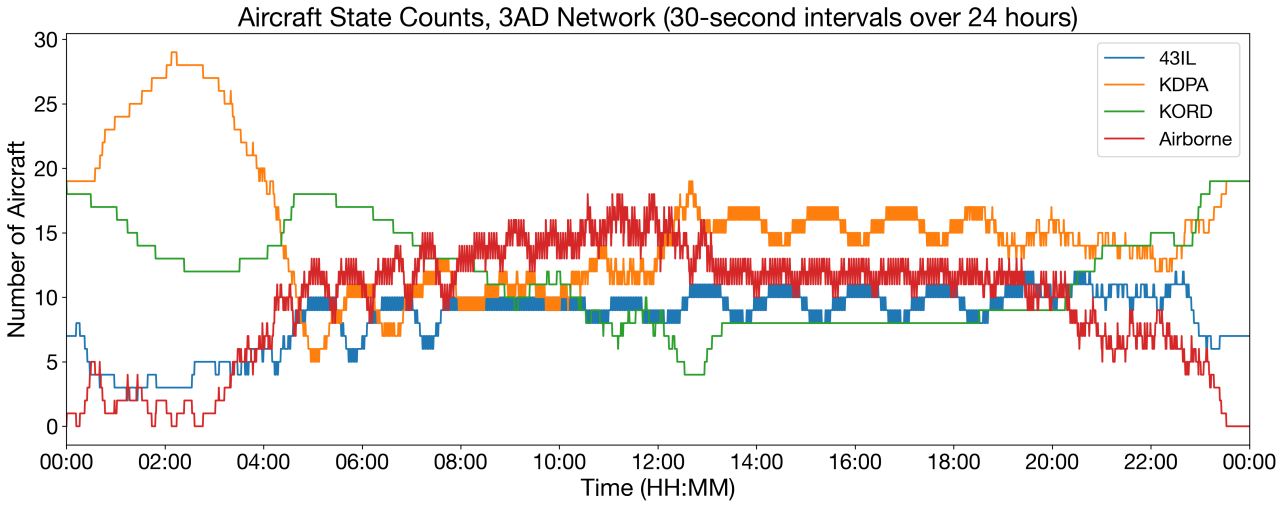


Figure 5 – Aircraft state counts at 30-second intervals throughout the 24-hour 3AD space-time network.

To examine whether AOG capacity limits specific to each aerodrome are adhered to, Fig. 6 presents AOG count variations across all aerodromes in the 3AD network throughout the simulation horizon. Figure 6 demonstrates that in the three-aerodrome network, none of the aerodromes violate AOG capacity limits, which also include the lower bound of zero aircraft on ground. In the case of 43IL (Vertiport Chicago FBO), its maximum AOG capacity limit of 12 was attained intermittently for a cumulative duration of 18 minutes between 19:27:00 and 22:40:30.

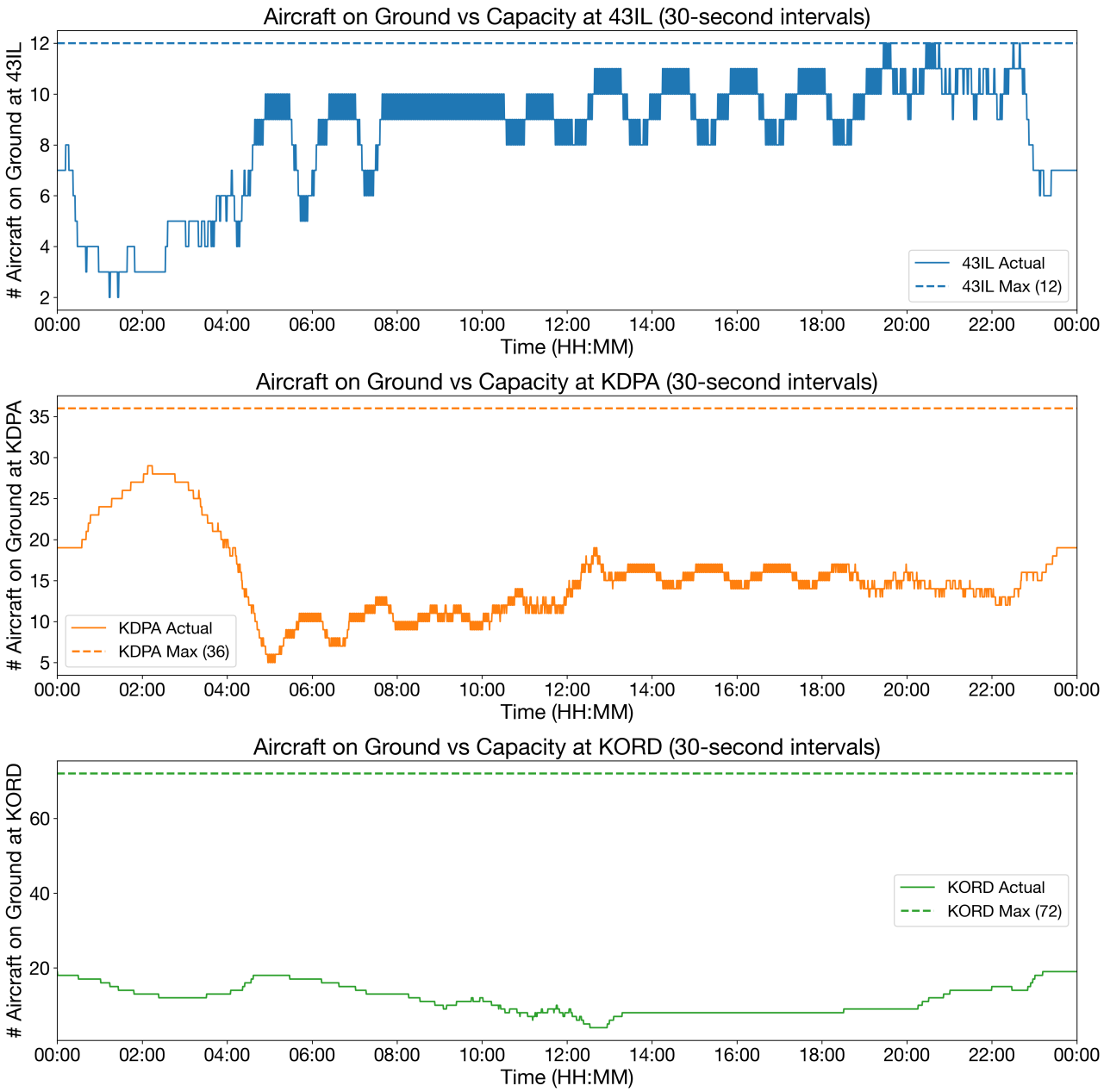


Figure 6 – Number of aircraft on ground across all aerodromes in the 3AD network at 30-second intervals.

5.2 Four-Aerodrome Networks

This study also considers two distinct four-aerodrome networks, both of which are augmentations of the 3AD network. The first (4AD-1) network includes Bollingbrook's Clow International Airport (1C5), whereas the second (4AD-2) includes Tinley Park Helistop (TF8).

On an effective-cost basis with four-passenger UAM flights, the UAM-preferring demand for the 4AD-1 network amounts to 71,728 individuals, which is a notable increase over the 39,438 commuters preferring UAM in the 3AD network. Applying the scheduled UAM model to the 4AD-1 network resulted in 3,104 passengers flown on 776 four-passenger flights, 97 additional passengers flown on 30 revenue repositioning flights, and 11 empty deadhead flights. Overall, the 4AD-1 network sees a total of 3,201 UAM passengers representing 4.46% of UAM-preferring demand, 817 flights with an average load factor of 97.9%, and a minimum fleet size of 44 aircraft. The 3,201 UAM passengers is an increase over the 2,976 in the 3AD network simulation.

The 4AD-2 network yields a UAM-preferring demand of 63,484 individuals, which also exceeds the 3AD network prediction and is slighly below the 4AD-1 network prediction. Unlike the 3AD and 4AD-1 networks, where Vertiport Chicago FBO (43IL) has the strictest AOG capacity-constrained aerodrome at 12 aircraft, the most capacity-constrained aerodrome in the 4AD-2 network is the Tinley Park Helistop (TF8), whose AOG capacity is just eight aircraft. This lower AOG capacity at the most "bottlenecked" aerodrome may have implications for the extent of UAM demand capture within the scheduled UAM operation. Applying the scheduled UAM model to the 4D-2 network, we obtain 715 four-passenger flights carrying 2,860 passengers, 22 revenue repositioning flights carrying 68 additional passengers, along with 10 empty deadhead flights. Altogether, the 4AD-2 network sees a total of 2,928 passengers representing 4.61% of UAM-preferring demand, 747 flights with an average load factor of 98.0%, and a minimum fleet size of 42 aircraft.

The addition of the TF8 aerodrome in the 4AD-2 network reduces the number of passengers carried by the scheduled UAM service relative to the 3AD network. This is likely because a greater share of UAM-preferring passengers are routed through TF8 (i.e., the shortest distance approach sends the commuter to TF8 rather than to a slightly further aerodrome from which they would still have a lower effective cost trip than a car-only trip) and subsequently subjected to its more restrictive capacity limits, thereby reducing the extent to which UAM demand can be accommodated across the network. More broadly, this illustrates an emergent property of scheduled UAM operations, whereby capacity limitations at the most constrained aerodrome propagate throughout the system and ultimately influence network-wide UAM demand capture. TF8 remains within its AOG capacity limit throughout the 24-hour simulation horizon, as shown in Fig. 7. Similarly, all aerodromes across both the 4AD-1 and 4AD-2 network scenarios remain within their respective AOG capacity limits throughout the simulation horizon while restoring the initial aircraft distribution at the end of each day.

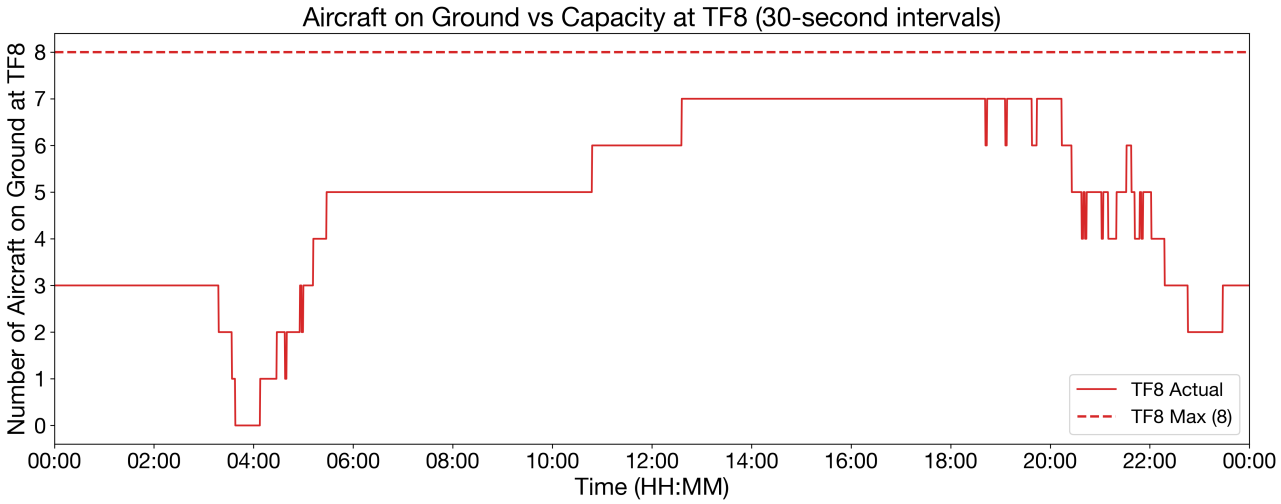


Figure 7 – Number of aircraft present throughout the day at the Tinley Park Helistop (TF8) aerodrome in the 4AD-2 network at 30-second intervals.

5.3 Summary of Results

Table 3 summarizes key performance metrics across the aerodrome networks considered in this work. We observe that across the three distinct aerodrome network scenarios, the scheduled UAM model converged to similar average load factors, fleet sizes, and the average number of flights per aircraft. The favorable average load factors observed across the aerodrome networks are attributed largely to the four-passenger heuristic in the schedule design methodology, which generates an overwhelming majority of flights.

Despite a high concentration of UAM demand around peak commuting periods, the resulting flight schedules and individual aircraft assignment support aircraft activity throughout much of the day. For

Table 3 – Summary of operational results across aerodrome networks. All metrics correspond to a daily operation unless stated otherwise.

Metric	**3AD**	**4AD-1**	**4AD-2**
UAM-preferring demand	39,438	71,728	63,484
Passengers carried	3,122	3,201	2,928
Demand captured (%)	7.92%	4.46%	4.61%
Total flights	794	817	747
Regular revenue (4-pax)	744	776	715
Repositioning revenue	43	30	22
Deadhead	7	11	10
Average load factor (%)	98.3%	97.9%	98.0%
Minimum fleet size	45	44	42
Average flights per aircraft	17.64	18.57	17.79
Average flight-hours per aircraft			
Among passenger flights			
Per day	5.465	5.758	5.572
Per year	1,366	1,440	1,393
Among all flights			
Per day	5.502	5.818	5.636
Per year	1,376	1,455	1,409

example, in the 3AD network as illustrated in Fig. 5, we observe that at least ten aircraft are airborne over a combined 11.5-hour period between 08:00:00 and 19:30:00. Furthermore, Table 3 shows that, across all aerodrome networks considered, aircraft collectively operate an average of no fewer than 17 passenger-carrying flights per day. This level of flight activity is reflected in average aircraft utilization, also summarized in Table 3 on both a daily and yearly basis, and measured in flight-hours for both passenger-carrying flights and all flights including empty deadheads.

Daily aircraft utilization values are calculated from an aggregation of the durations between lift-off and touchdown across all flights and aircraft, and then divided by the fleet size. Because empty deadheads represent only a small fraction of total operations, there is little difference between aircraft utilization figures with and without them. To annualize aircraft utilization, we assume 250 days of UAM operations based on Kohlman et al. [51], which is consistent with the commute-trip demand modeled in this study. Annual aircraft utilization values of approximately 2,000 flight-hours are commonly assumed in the literature for assessments of eVTOL aircraft direct operating costs (DOC), such as those of Kohlman et al. [51] and Uber Elevate [52]. For the present study, multiplying the daily aircraft utilization in flight-hours by 250 business days yields yearly average aircraft utilization values ranging between 1,350 and 1,450 flight hours across the aerodrome networks.

Collectively, the results presented in this section demonstrate that the schedule design and tail-number assignment methodology utilized and enhanced in this study can be successfully applied and scaled to larger aerodrome networks while maintaining adherence to AOG capacity constraints across all aerodromes and a repeatable daily schedule of operations. The results further illustrate that both the selection and geographic placement of aerodromes can influence potential UAM demand substantially and the resultant UAM demand capture achieved by a scheduled UAM service. Although the present study does not seek to evaluate the relative merits of one aerodrome location or network configuration over another, the differences observed between the aerodrome networks demonstrate the sensitivity of scheduled UAM operations to aerodrome network design choices.

6. Conclusions and Future Work

This study presented a framework for schedule-based UAM operations representing a hypothetical operator providing reservation-based, timetable-bound services. Building upon Ref. [18], the commercial-airline-like methodology combines schedule design with tail-number assignment and, when applied to both three- and four-aerodrome networks in the Chicago metropolitan area, the methodology successfully produced feasible, repeatable daily flight schedules while effectively minimizing fleet size and respecting aerodrome aircraft-on-ground (AOG) capacity constraints. Across all aerodrome network scenarios considered, the resulting schedules yielded average load factors of approximately 98% with four-passenger revenue flights comprising the overwhelming majority of operations, while aircraft collectively operated at least 17 passenger-carrying flights per day and achieved annual utilization figures in excess of 1,350 flight-hours. Other principal findings and implications of the study have been summarized in Section 5.3.

The methodology presented and results obtained in this study rely upon several assumptions and modeling abstractions described in Sections 3. and 4., many of which motivate directions for future research. First, the strict four-passenger heuristic currently used to group passengers into flights can be relaxed to allow flights with fewer passengers, paired with a prioritization mechanism that favors higher-occupancy flights when a conflict arises for the same departure or arrival slots. Such an extension would likely require additional consideration of ticket pricing and profitability, particularly for lower-occupancy flights.

Second, the scheduled UAM model presented in this study was intentionally formulated around a 24-hour simulation horizon and a repeatable daily schedule of operations. Consequently, end-of-day RTB repositioning flights are required to restore the initial aircraft distribution at the conclusion of each day. Future work may extend the simulation horizon beyond 24 hours to represent an entire workweek, thereby allowing individual aircraft to operate different flight-strings on different days and potentially reducing the need for some repositioning flights. Such an extension would also enable verification of whether flight activity could distributed more evenly across the fleet, which is important for maintenance planning. Along similar lines, future work may incorporate maintenance routing and battery charging considerations directly into the tail-number assignment mechanism, recognizing that not all aerodromes may offer maintenance or charging facilities.

Third, the tail-number assignment methodology may be reformulated using a branch-and-price framework following Barnhart et al. [46], enabling a more rigorous treatment of flight-string generation for aircraft assignments and fleet-size minimization. Repositioning flights could then emerge directly from the optimization framework rather than being generated through post-processing, while explicitly and simultaneously accounting for aerodrome capacity constraints at both the departure and arrival aerodromes. Furthermore, annual aircraft utilization metrics derived from the resulting flight-strings may be integrated with existing eVTOL direct operating cost models to better connect scheduling outcomes with the economic performance of a scheduled UAM operator.

The cost models for the UAM ticket price and for the fully-burdened (including maintenance and wear-and-tear) car travel cost per mile, as well as the assumption that the value of time for commuters is equal to their equivalent hourly pay, all play an important and significant role in predicting the number of UAM-preferred trips.

Additional avenues for future research include more detailed modeling of aerodrome infrastructure capabilities and limitations to better identify potential operational bottlenecks, comparisons between scheduled and on-demand UAM service models particularly based on metrics outlined in Section 5.3, and the consideration of off-nominal events such as adverse weather and system failures. Finally, the methodology presented in this study may be applied to other metropolitan areas to further investigate the operational performance of scheduled UAM services under different demand and aerodrome network characteristics.

7. Contact Author Email Address

mailto: aedsel@purdue.edu

8. Copyright Statement

Copyright © 2026 Adler Edsel, William A. Crossley, and Daniel A. DeLaurentis. The authors also confirm that they have obtained permission, from the copyright holder of any third party material included in this paper, to publish it as part of their paper. The authors confirm that they give permission, or have obtained permission from the copyright holder of this paper, for the publication and distribution of this paper as part of the ICAS proceedings or as individual off-prints from the proceedings.

References

[1] David P Thipphavong, Rafael Apaza, Bryan Barmore, Vernol Battiste, Barbara Burian, Quang Dao, Michael Feary, Susie Go, Kenneth H Goodrich, Jeffrey Homola, et al. Urban air mobility airspace integration concepts and considerations. In *2018 Aviation Technology, Integration, and Operations Conference*, page 3676, 2018.

[2] A. Pukhova, C. Llorca, A. Moreno, C. Staves, Q. Zhang, and R. Moeckel. Flying taxis revived: Can urban air mobility reduce road congestion? *Journal of Urban Mobility*, 1:100002, 2021.

[3] Xuan Jiang, Yuhan Tang, Junzhe Cao, Vishwanath Bulusu, Hao (Frank) Yang, Xin Peng, Yunhan Zheng, Jinhua Zhao, and Raja Sengupta. Simulating integration of urban air mobility into existing transportation systems: Survey. *Journal of Air Transportation*, 32(3):97–107, 2024.

[4] Joby Aviation, Inc. Joby, nasa simulation demonstrates up to 120 air taxi operations per hour in busy airspace, 2023. Accessed July 4, 2025.

[5] Greater Orlando Aviation Authority. Orlando international taking steps in future vertiport development, 2025. Accessed July 4, 2025.

[6] Delta Air Lines and Joby Aviation, Inc. Delta, joby aviation partner to pioneer home-to-airport transportation to customers, 2022. Accessed July 4, 2025.

[7] Eve Air Mobility & United Airlines. United airlines and eve air mobility collaborating to bring first electric commuter flights to san francisco, 2023. Accessed July 4, 2025.

[8] Archer Aviation, Inc. and United Airlines. Archer unveils vision for new york air taxi network, including routes between manhattan and nearby airports in partnership with united airlines, 2025. Accessed July 4, 2025.

[9] Federal Aviation Administration (FAA). *Engineering Brief No. 105A: Vertiport Design, Supplemental Guidance to Advisory Circular 150/5390-2D, Heliport Design*. Federal Aviation Administration, 2024. Accessed July 4, 2025.

[10] UK Civil Aviation Authority. Groundbreaking roadmap for aircraft of the future released, 2025. Accessed July 4, 2025.

[11] U.S. Department of Transportation and Federal Aviation Administration. The future of aviation is here: Trump's transportation secretary sean p. duffy and faa unveil eight selections for pilot program testing next-gen aircraft in america's skies, 2026. Accessed June 12, 2026.

[12] Federal Aviation Administration. *Urban Air Mobility (UAM) Concept of Operations, Version 2.0*. Federal Aviation Administration, 2023. Accessed July 4, 2025.

[13] Mehdi Bennaceur, Rémi Delmas, and Youssef Hamadi. Passenger-centric urban air mobility: Fairness trade-offs and operational efficiency. *Transportation Research Part C: Emerging Technologies*, 136:103519, 2022.

[14] Nabih Naeem, Patrick Ratei, Prajwal Shiva Prakasha, Lukas Asmer, Roman Jaksche, Henry Pak, Karolin Schweiger, Asija Velieva, Fares Naser, Majed Swaid, Jan Pertz, and Malte Niklaß. A collaborative system of systems simulation of urban air mobility. *CEAS Aeronautical Journal*, 2024.

[15] The Boeing Company and Wisk Aero. *Concept of Operations for Uncrewed Urban Air Mobility*, September 2022.

[16] Syed Arbab Mohd Shihab, Peng Wei, Daniela Sofia Jurado Ramirez, Rodrigo Mesa-Arango, and Christina Bloebaum. By schedule or on demand? - a hybrid operation concept for urban air mobility. In *AIAA Aviation 2019 Forum*, page 3522, 2019.

[17] Jungu Kang and Sang Hyun Kim. Reserved or not? - scheduled urban air mobility services in a hub-and-spoke network. In *AIAA AVIATION FORUM AND ASCEND 2024*, page 4078, 2024.

[18] Adler Edsel. A study of aircraft scheduling and routing for urban air mobility service. Master's thesis, Purdue University, West Lafayette, IN, 2025.

[19] Mehdi Bennaceur, Rémi Delmas, and Youssef Hamadi. Passenger-centric urban air mobility: Fairness trade-offs and operational efficiency. *Transportation Research Part C: Emerging Technologies*, 136:103519, 2022.

[20] Shuting Yang, Jiazhen Zhou, Dengfeng Sun, and Daniel DeLaurentis. Ride-sharing with advanced air mobility. Technical report, Center for Connected and Automated Transportation, Purdue University, 2023.

[21] Qinshuang Wei, Gustav Nilsson, and Samuel Coogan. Scheduling of urban air mobility services with limited landing capacity and uncertain travel times. In *2021 American Control Conference (ACC)*, pages 1681–1686, 2021.

[22] Apoorv Maheshwari, Brandon E. Sells, Stephanie Harrington, Dan DeLaurentis, and William Crossley. Evaluating impact of operational limits by estimating potential uam trips in an urban area. In *AIAA AVIATION 2021 FORUM*, page 3174, 2021.

[23] The United States Census Bureau. LEHD Origin-Destination Employment Statistics. `https://lehd.ces.census.gov/data/`, 2023. Accessed: 2023-12-11.

[24] The United States Census Bureau. American Community Survey. `https://www.census.gov/programs-surveys/acs`, 2023. Accessed: 2023-12-11.

[25] Federal Highway Administration. National Travel Household Survey. `https://nhts.ornl.gov`, 2023. Accessed: 2023-12-11.

[26] OpenStreetMap Contributors. OpenStreetMap. `https://www.openstreetmap.org/copyright`, 2024. Accessed: 2024-04-12.

[27] TomTom. Tomtom traffic index. `https://www.tomtom.com/traffic-index/`, 2022. Accessed: February 24, 2024.

[28] Brandon E. Sells, Apoorv Maheshwari, Hsun Chao, Ethan Wright, William Crossley, and Dengfeng Sun. Evaluating the impact of urban air mobility aerodrome siting on mode choice. In *AIAA AVIATION 2021 FORUM*, page 2371, 2021.

[29] Brandon E Sells, Keshav Iyengar, Byeonghun Kim, Nick Gunady, Ethan Wright, Seejay R Patel, Daniel A DeLaurentis, and William A Crossley. A comparative study of aerodrome-related operational limits for passenger-carrying missions across metropolitans. In *AIAA AVIATION 2023 Forum*, page 3410, 2023.

[30] Internal Revenue Service. Standard mileage rates. `https://www.irs.gov/tax-professionals/standard-mileage-rates`, 2026. Accessed: 2026-06-12.

[31] Satadru Roy, Apoorv Maheshwari, William A. Crossley, and Daniel A. DeLaurentis. A study on the impact of aircraft technology on the future of regional transportation using small aircraft. In *2018 Aviation Technology, Integration, and Operations Conference*, page 3056, 2018.

[32] Satadru Roy, Apoorv Maheshwari, William A. Crossley, and Daniel A. DeLaurentis. A study to investigate total mobility using both ctol and vtol-capable aircraft. In *AIAA AVIATION 2019 Forum*, page 3518, 2019.

[33] Apoorv Maheshwari, Sai Mudumba, Brandon E. Sells, Daniel A. DeLaurentis, and William A. Crossley. Identifying and analyzing operations limits for passenger-carrying urban air mobility missions. In *AIAA AVIATION 2020 FORUM*, page 2913, 2020.

[34] Satadru Roy, Apoorv Maheshwari, William A Crossley, and Daniel A DeLaurentis. Future regional air mobility analysis using conventional, electric, and autonomous vehicles. *Journal of Air Transportation*, 29(3):113–126, 2021.

[35] Adler Edsel, Somrick Das Biswas, Michael Kilbourne, Rishikesh Gadre, Spruha Vashi, Kshitij Mall, William A Crossley, Daniel A DeLaurentis, Michael D Patterson, and Brandon E Sells. Exploring ridesharing in passenger urban air mobility: A comparative analysis. In *34th Congress of the International Council of the Aeronautical Sciences*, 2024.

[36] Somrick Das Biswas, Jonah Gerardus, Kshitij Mall, Daniel A DeLaurentis, William A Crossley, Michael D Patterson, and E Sells, Brandon. Initial estimation of the number of urban air mobility operations at aerodromes to assess operational limits. In *AIAA AVIATION 2025 Forum*, page 3780, 2025.

[37] Adler Edsel, Somrick Das Biswas, Spruha Vashi, Kshitij Mall, William A. Crossley, Daniel A. DeLaurentis, Michael D. Patterson, and Brandon E. Sells. Evaluating potential carbon emissions operational limits on urban air mobility with ridesharing. *Journal of Air Transportation*, 2026. Accepted for publication.

[38] Census Reporter. Chicago-Naperville-Elgin, IL-IN Metro Area, 2026. Accessed: 2026-06-10.

[39] Census Reporter. Chicago-Naperville, IL-IN-WI Combined Statistical Area, 2026. Accessed: 2026-06-10.

[40] AirNav: KORD – Chicago O'Hare International Airport, 2024. Accessed: 2025-07-08.

[41] AirNav: 43IL – Vertiport Chicago FBO, 2024. Accessed: 2025-07-08.

[42] AirNav: KDPA – Dupage Airport, 2024. Accessed: 2025-07-08.

[43] AirNav: 1C5 – Bollingbrook's Clow International Airport, 2025. Accessed: 2026-06-10.

[44] AirNav: TF8 – Tinley Park Helistop, 2025. Accessed: 2026-06-10.

[45] Christopher A. Hane, Cynthia Barnhart, Ellis L. Johnson, Roy E. Marsten, George L. Nemhauser, and Gabriele Sigismondi. The fleet assignment problem: Solving a large-scale integer program. *Mathematical Programming*, 70(1):211–232, 1995.

[46] Cynthia Barnhart, Natashia L. Boland, Lloyd W. Clarke, Ellis L. Johnson, George L. Nemhauser, and Rajesh G. Shenoi. Flight string models for aircraft fleeting and routing. *Transportation Science*, 32(3):208–220, 1998.

[47] Peter P. Belobaba, Amedeo R. Odoni, and Cynthia Barnhart, editors. *The Global Airline Industry*. Aerospace Series. Wiley-Blackwell, Chichester, West Sussex, 2015.

[48] Parker D Vascik. *Systems Analysis of Urban Air Mobility Operational Scaling*. PhD thesis, Massachusetts Institute of Technology, 2020.

[49] John R. Dermody. Advisory circular 150/5390-2d: Heliport design. Technical Report AC 150/5390-2D, U.S. Department of Transportation, Federal Aviation Administration, 1 2023. Accessed: 2025-05-01.

[50] Level 3 airports: Slot administration and schedule facilitation, 2024. Accessed: 2025-07-08.

[51] Lee W. Kohlman, Michael D. Patterson, and Brooke E. Raabe. Urban air mobility network and vehicle type—modeling and assessment. Technical Report NASA/TM-2019-220072, National Aeronautics and Space Administration, Moffett Field, California, February 2019.

[52] Jeff Holden and Nikhil Goel. Uber elevate: Fast-forwarding to a future of on-demand urban air transportation, 2016. Accessed: 2024-05-31.